

## Synthesis of new granular surfactant iron pillared montmorillonite with gluten: application to the removal of cationic dyes in mixture systems

Amel Louadj, Omar Bouras, Benamar Cheknane\*, Faiza Zermane

Laboratoire Eau Environnement et Développement Durable, Faculté de Technologie, Université Saad Dahlab-Blida 1, BP 270, 09000 Blida, Algérie, Tel. (213) 0553348944, email: louadjamel@yahoo.fr (A. Louadj), Tel. (213) 0555906864, email: o.bouras@yahoo.fr (O. Bouras), Tel. (213) 0773317601, email: b.cheknane@yahoo.fr, ocheknane@yahoo.fr (B. Cheknane), Tel. (213) 0770134087, email: faizazermane@yahoo.fr (F. Zermane)

Received 21 April 2017; Accepted 21 October 2017

### ABSTRACT

A series of novel resistant granular sorbents based on iron granular surfactant modified pillared montmorillonite and gluten as binder noted (Fe-GSMPM) are prepared and used in adsorption towards hydrosoluble micropollutants. The batch sorption of Malachite Green (MG) and/or Rhodamine B (RB) both on single and binary component systems from aqueous solutions was investigated. In all used component systems, sorption capacities were depending both on the pH and the granule size. In single component systems, results showed that sorption on Fe-GSMPM are very effective and more quickly with MG than RB with obtained amounts reached more than 9 and 6 mg/g at pH = 6 and strongly decreased more than 3 mg/g for both solutes at pH = 3, respectively. In binary component systems at different weight ratios  $r$  (MG/RB = 1/9, 1/3, 1, 3 and 9) and at pH 6, the sorption capacities decreased significantly with values lower than those obtained in single-component systems. Isotherms were best described using the Freundlich model in single component systems with  $R^2$  reach 0.9. In binary mixture systems, results indicate that the Sheindorf–Rebhun–Sheintuch (SRS) model provides the best correlation of the experimental data by the higher competition coefficients, which increase with decreasing weight MG/RB ratio.

*Keywords:* Granulation; Adsorption; Binder; Malachite green; Rhodamine B

### 1. Introduction

Water pollution by organic compounds such as textile dyes, even in trace amounts, is a major environmental problem because of their toxicity, the complexity of their chemical structures and especially their low biodegradability. *Textile effluents contain both Malachite Green (MG) and Rhodamine B (RB) presents effect on the human health and environment* [1]. Their concentrations in the effluents should be controlled in order to respect environment norms and legislation on water quality which become more stringent actually. That is why this kind of pollution is now a source of an environmental degradation and causes currently a worldwide interest [1–5]. On the other hand, the technological and industrial development has caused major changes

in the various physico-chemical methods of decontamination of polluted waters [6–9].

The wastewaters rich in dangerous pollutants such as dyes, paint, detergents that cannot be removed by conventional treatment systems are generally generated by various industries.

Among these methods, adsorption on porous materials such as activated carbons AC remains the most commonly used. Sorption on natural clays, which represents an efficient and cheaper separation method, has been developed to study the interaction mechanisms of pollutants by bentonites due to their both low permeability and interesting rheological properties [10–16].

In the past, several research papers were dedicated to synthesis a new generation of organophilic material adsorbent powders based on clays. Various synthesized inorga-

\*Corresponding author.

no-organo clays complexes (named also surfactant modified pillared clays) proved their high sorption efficiencies especially in single component systems towards several organic compounds in polluted water.

Despite the high performance of the clays materials in batch adsorption systems, their use in dynamic systems presents several disadvantages associated to the size of their particles that are often very small ( $d_p < 50 \mu\text{m}$ ). Furthermore, these finely divided materials are also confronted to the difficult solid liquid separation against the treated water [17–23]. Few years ago, many researchers have demonstrated that modified powdered clays could be shaped as gel-like beads by encapsulation [24] or as granules by wet granulation [5].

The idea of turning the powder into pellets or granules fits into the new water treatment philosophy because of problems caused by colloidal montmorillonite which, despite its cation exchange capacity and high specific surface area cannot be used in dynamic mode [25].

Some previous works [5,25] have shown that agglomeration of some inorgano-organo pillared clays powder by wet granulation could increase their mechanical properties (bulk density, porosity, hardness, compressibility) and thus enhance the field of applications of the resulting solids in water treatment.

In this way, three different techniques may be used for the preparation of the mixture before the compressing step: direct compression, dry granulation or wet granulation. Direct compaction method is ideal for powders which may be mixed well and does not require further granulation step prior introduction into the tablet press [26–30].

Based on the same approach, this study is conducted to shape a powder mixtures containing iron surfactant modified pillared montmorillonite noted (Fe-SMPM) and gluten (viscoelastic binder obtained by leaching a wheat dough) using dry granulation by compaction in order to obtain the granular sorbents noted (Fe-GSMPM).

The granulation method allows both the structure of solid fine powders in agglomerated particles of almost specific shapes, and ameliorates the physical properties in terms of density, porosity, hardness, compressibility, and thus facilitates their use in the field of water treatment by adsorption in dynamic mode [31–39]. Furthermore, it avoids the production of undesirable non-pulp and which may form for injection in the case of a wet granulation between gluten and water.

In order to understand the behavior of these new generations of granules sorbents based on compression-granulated iron bridged montmorillonite using gluten as a novel inert binder, we investigated the sorption of MG and RB in both single and binary-component systems from aqueous solutions. All kinetic and sorption isotherms were studied at various pH, granules size and MG/RB weight ratio values.

The novelty of this study is in the aggregation of the modified clay particles by gluten as an inert binder in order to prepare resistant and uniform Fe-GSMPM grains using the compaction granulation method. This new generation of Fe-GSMPM grains could be used in the packing of column beds to be used in the dynamic adsorption of organic and/or inorganic pollutants.

In fact, this type of granules provides a texture and rigidity in favor of the investigation on dynamic adsorption

contrary to the powder materials that block the liquid flow by clogging phenomenon, hence industrial interest.

## 2. Experimental

### 2.1. Solid sorbent powders

Obtained Na-montmorillonite noted Na-Mt used as starting material was prepared by purification of crude bentonite (Roussel site in Maghnia- west of Algeria). Its characteristics and its purification mode were according to the protocol described in some works earlier [40,41].

The intercalation of Na-Mt by the iron pillaring solution was obtained with the optimal following parameters according to the method described previously by [41–43]:

Final concentration of iron  $[\text{Fe}]_f = 0.2 \text{ M}$ , Molar ratio  $\text{OH}/\text{Fe} = 2$ ,  $\text{Fe}/\text{Na-Mt} = 5 \text{ mmol/g}$ .

Fe-SMPM was synthesized as follow according to the methods described in some works previously [40,42] and given as follows.

A cetyl trimethyl ammonium bromide noted CTAB (Biochem chemopharma, purity > 99%) was used without further purification in deionized water to prepare an aqueous solution at 0.2% (w/w).

In order to increase the hydrophobicity of the final sorbent Fe-SMPM, a suspension of iron pillared montmorillonite (0.5%) was treated with CTAB 2 g/L (0.5%, w/w) at room temperature of  $20 \pm 2^\circ\text{C}$ . The final obtained solid, named Fe-SMPM, was separated by vacuum filtration, washed several times by deionized water, dried at  $40^\circ\text{C}$  for at least 48 h and finally ground ( $<50 \mu\text{m}$ ) and protected from light.

The granulation of Fe-SMPM powder (*the size is less than  $50 \mu\text{m}$* ) is realized by mixing with gluten as a binder to obtain resistant, strength and consistency granules designated by Fe-GSMPM.

The gluten used is extracted from wheat by continuous treatment with a concentrated solution of NaCl (25 g/L). This chemical treatment is continued until the liquid becomes transparent. Gluten obtained by drying at room temperature ( $20 \pm 2^\circ\text{C}$ ) for a period of 48 h is stored in a dark bottle before use in compaction granulation process.

#### 2.1.1. Granulation procedure

All steps of modified clay granulations are presented in Fig. 1. An initial mass of 12 g of Fe-SMPM was firstly mixed with 8 g of gluten powder at desired weight ratio (6/4; w/w), because a mechanical resistance of Fe-SMPM granules increased with binder concentration and a maximum was attained for 40%, such as (6/4, w/w).

All obtained mixtures were homogenized using mechanical shaker and then compressed to form dense, compact disks, ranging in size from between few millimeters and several centimeters [14].

The granulation process is done by controlling the spitting mixture, as it passes through two rotating wheels in the opposite direction at 2.5 rpm speed for 24 s.

The sharing of gluten particles to those of Fe-SMPM fine powder allows coalescence between the various parti-

cles through nucleation such as proposed by some authors previously [2,4].

The protocol of the granules formation is summary in Fig. 1.

### 2.1.2. Characterization of sorbents

A granulometric analysis is realized by a granulometer (VEB Metallwaber Meustadl/Betrieb des VEB kombinat NAGEMA) equipped with several sieves diameters ranging from 20  $\mu$  to several mm.

The disintegration tests were carried out at room temperature ( $25 \pm 2^\circ\text{C}$ ), stirrer speed of 200 rpm and during 24 h in a mechanical shaker containing 200 mL of deionized water. Each sample of six granules was immersed in a shaker to undergo disintegration by the end of the test indicates the solids to be resistant.

The friability tests were performed using a friabilator apparatus (VWR, model VMS-AS40).

A sample of twenty granules was initially weighted ( $m_1$ ) and run into a drum operating at a stirring speed of 25 rpm for a period of 10 min.

Obtained granules were weighted ( $m_2$ ) and friability (%) was calculated according to Eq. (1).

$$F(\%) = \frac{(m_1 - m_2)}{m_1} \times 100 \quad (1)$$

where  $m_1$  represent the initial weight, and  $m_2$  the weight after friability.

The zetametry is a method to predict the reactivity of solid supports and their electrophoretic mobility at various pH.

The principle of zetametry is to cause the movement of the particles in suspension under the action of an electric field. The electronic potentials of studied various suspensions were measured using a zetaphoremeter IV model Z4000 (CAD Instruments).

The determination of the surface charge of Fe-GSMPM sorbents allows predicting the different interactions between adsorbent surface sites and adsorbate molecules.

$\text{pH}_{\text{pzc}}$  is the point of zero charge of the surface, the charge of adsorbent surface is positive at a solution pH lower than  $\text{pH}_{\text{pzc}}$  and is negative at a solution pH higher than  $\text{pH}_{\text{pzc}}$ .

The crystalline structure of samples was determined by X-ray diffraction (XRD) recorded on a Siemens D-5000 X-ray powder diffractometer (Cu  $K\alpha$  radiation,  $k = 1.5418 \text{ \AA}$ ). Specific Surface Area (SSA) values were calculated from the BET isotherm plots. FT-IR spectroscopy (using a Perkin Elmer FT 310 FTIR spectrometer) was performed to identify the chemical functional groups present in the samples. The substance was finely ground and dispersed into KBr powder-pressed pellets. IR Transmittance data were obtained over a range of wavenumbers from 4000 to  $400 \text{ cm}^{-1}$ . Solid morphology of granules was determined by scanning electron microscopy (Philips XL30 with EDS, and EPMA CAMECASX 100).

## 2.2. Adsorption procedure

### 2.2.1. Sorbate solutions

All used chemicals were of analytical grade and used without any pretreatment or purification.

Stock solutions of 1 g/L of both Malachite Green (Fluka, purity: 99%) and Rhodamine B (BDH chemicals Ltd, purity: 99%) were prepared by dissolving the appropriate amount of each product in deionized water (resistivity  $> 18 \text{ M}\Omega\cdot\text{cm}$ ; dissolved organic carbon less than 0.2 mg/L) at room temperature ( $20 \pm 2^\circ\text{C}$ ).

The main physicochemical characteristics of the two used dyes are listed in Table 1.

Working dyes solutions (stock and diluted solutions of 10 mg/L of MG and RB) were then kept in brown flasks at room temperature in the dark to prevent any possible dye photodegradation.

The choice was done for the single and binary systems, and this so that we can compare with dynamic sorption, because at higher concentrations it cannot illustrate pierces curve.

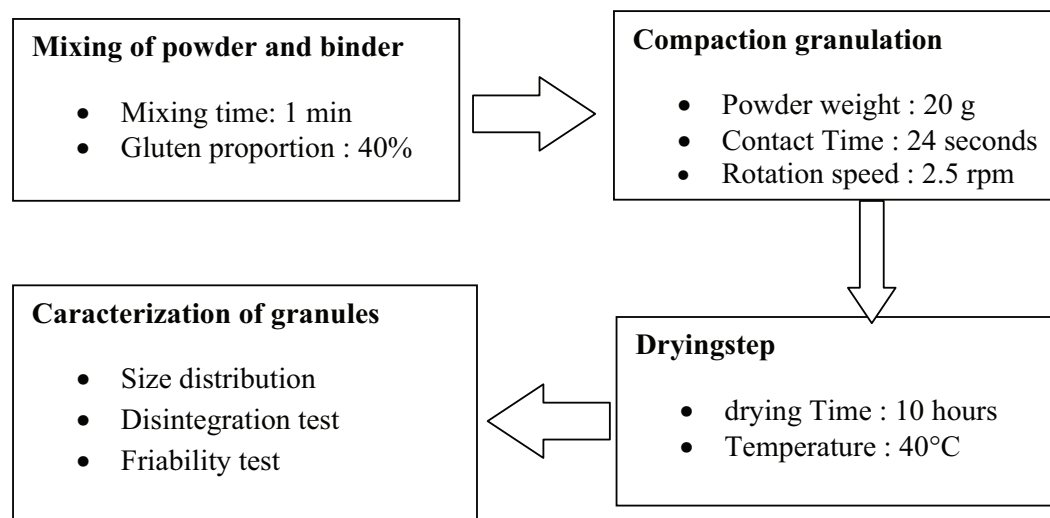
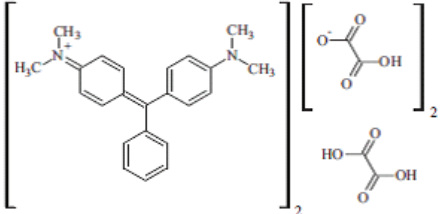
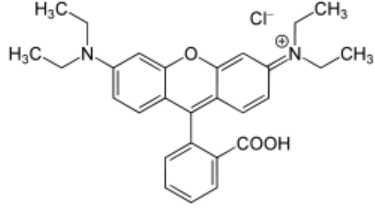


Fig. 1. Steps of preparation of Fe-GSMPM by compaction granulation.

Table 1  
Physicochemical characteristic of the used dyes

Dyes	MG	RB
		
Chemical formula	$C_{23}H_{25}ClN_2$	$C_{28}H_{31}ClN_2O_3$
N°CAS	18015-76-4	81-88-9
Mw (g/mol)	$364.91 \pm 0.023$	$479.01 \pm 0.028$
pKa	10	4.42
Solubility (g/L) at 20°C in water	–	50
$\lambda_{max}$ (nm)	616	553

The appropriate wavelengths of MG and RB were obtained by scanning each dye solution from 200 to 800 nm using the Spectrophotometer model Shimadzu 170 UV/visible.

### 2.2.2. Sorption kinetics

Kinetic studies in batch systems of MG and/or RB were studied both in single and binary systems in order to investigate the mechanism of adsorption as a function of contact time and to determine the required time to get equilibrium.

Experiments were conducted at room temperature  $20 \pm 2^\circ\text{C}$  and at pH 6 in a series of 40 identical brown flasks by shaking 0.1 g of Fe-GSMPM granules ( $800 < \Phi < 1200 \mu\text{m}$ ) with 100 mL of the dye solution (100 mg/L) at a constant speed of 200 rpm on a horizontal mechanical shaker (Ikalabortechnik model KS 501).

In order to optimize the contact time, a 100 mL was sampled in a separated flask at a chosen time from 0 to 1200 min and then filtered through 0.45  $\mu\text{m}$  Sartorius cellulose nitrate filter.

The final concentrations of MG and/or RB in supernatants were determined using 1 cm quartz cell with a UV-visible spectrophotometer at the appropriate wavelength  $\lambda_{max}$  values of 617 and/or 553 nm for MG and RB, respectively.

These analyzes are carried out 3 times in order to take a representative average in order to ensure the reproducibility of the results.

### 2.2.3. Sorption isotherms in single component systems

Similar conditions were conducted to study the uptake of MG and/or RB molecules onto Fe-GSMPM.

According to some previous studies on the adsorption of dyes on modified clays [5,42], the pH of all aqueous suspensions was chosen as selective parameter for further experiments and maintained at pH 6 by adding few drops of NaOH or HCl (0.01 N).

Isotherms studies were conducted by shaking different quantities of granular sorbent Fe-GSMPM (varying from 10

to 100 mg) with 100 mL of dye solution (10 mg/L) at room temperature ( $20 \pm 2^\circ\text{C}$ ) and at 200 rpm on a horizontal mechanical shaker (Ikalabortechnik model KS 501).

After an equilibrium time of 24 h, the content of each flask was then filtered through 0.45  $\mu\text{m}$  Sartorius membrane filter, and the concentrations in all supernatants were then determined spectrophotometrically at appropriate wavelengths of MG and/or RB.

Experiments were duplicated, with blanks (constituted without Fe-GSMPM and/or without dye) and were conducted simultaneously at similar conditions to account for experimental conditions.

The sorption data were fitted using the Freundlich equation, which is the approximate global form of the Langmuir local sorption isotherm.

In accordance with previous results [5], isotherms data were analyzed by using the Freundlich equation:

$$q_e = K_F C_e^n \quad (2)$$

where  $q_e$  (mg/g) is the amount of sorbed compound,  $C_e$  (mg/L) the equilibrium concentration,  $K_F$  ( $\text{mg}^{(1-1/n)} \text{L}^{1/n} / \text{g}$ ) the affinity coefficient related to the sorptive capacity, and  $n$  an estimated sorptive intensity or surface heterogeneity parameter.

The unknown constants in this model equation are obtained using nonlinear least-squares data processing by the Origin 8.0 software at the 95% confidence level.

### 2.2.4. Sorption isotherms in binary component systems

In binary mixture systems, similar experiments were conducted to study the uptake of MG and/or RB molecules onto Fe-GSMPM.

Isotherms of each solute were derived by shaking different quantities of Fe-GSMPM (varying from 10 to 100 mg) with 100 mL of solution containing MG and/or RB.

For the sorption selectivity studies, experiments were performed at different (MG/RB) weight ratios (1/9, 1/3, 1, 3 and 9) and only at pH 6. Since the main objective herein is

to examine the mutual influence of MG and RB, the initial concentration of MG in all mixtures was set at 10 mg/L.

Each experiment was duplicated, with blanks constituted without sorbent and/or without sorbate.

Supernatants from the (MG/RB) solutions were obtained by the same conditions as described above.

In binary component systems, interferences and competitions phenomena will take place between the molecules of GM and RB towards the adsorbent surface sites. That is why; we have applied both the correction for the spectrophotometric determination of residual concentrations by using Eq. (3) and the Sheindorf-Rebhun-Sheintuch (SRS) model [42], whose equations are the following:

$$C_{MG} = \frac{K_{RB2}d_{\gamma1} - K_{RB1}d_{\gamma2}}{K_{MG1}K_{RB2} - K_{MG2}K_{RB1}} \tag{3}$$

$$C_{RB} = \frac{K_{MG1}d_{\gamma2} - K_{MG2}d_{\gamma1}}{K_{MG1}K_{RB2} - K_{MG2}K_{RB1}}$$

where  $(C_{MG}, C_{RB})$ ;  $(K_{MG1}, K_{MG2}, K_{RB1}, K_{RB2})$ ;  $(d_{\lambda1}, d_{\lambda2})$  are respectively the concentration of MG and RB, the calibration constants for the dyes at their characteristic adsorption wavelengths, and the optical densities at the two wavelengths  $\lambda_1$  and  $\lambda_2$ .

$$Qe_{MG} = K_{MG}Ce_{MG}(Ce_{MG} + a_{12}Ce_{RB})^{n_{MG}-1} \tag{4}$$

$$Qe_{RB} = K_{RB}Ce_{RB}(Ce_{RB} + a_{21}Ce_{MG})^{n_{RB}-1}$$

where  $a_{12}$  and  $a_{21}$  are the competition coefficients (interaction parameters) of MG vs. RB and RB vs. MG, respectively;  $K_{MG}, K_{RB}, n_{MG}$  and  $n_{RB}$  are Freundlich equation constants [see Eq. (4)] obtained from the respective single-component isotherms.

Competition coefficients  $a_{12}$  and  $a_{21}$  were determined by running the STATISTICA software with iterative method: Simplex-Newton, with the additional constraint of respecting:  $a_{12} \times a_{21} = 1$  [44].

The coefficient formula RMSE (Root Mean Square Error) was used to evaluate all these results with Eq. (5).

$$RMSE = \sqrt{\frac{1}{N} \sum_{i=1}^N [Q_{theoretical} - Q_{experimental}]^2} \tag{5}$$

where  $Q_{theoretical}$  is the sorption quantities calculated with Eq. (4) and  $Q_{experimental}$  is the sorption quantities experimental.

### 3. Results and discussion

#### 3.1. Characterization of prepared granules

##### 3.1.1. Granulometric analysis

According to Fig. 2, the particle size analysis of the prepared Fe-GSMPM sorbents seems to be mixtures of two different classes. The first one between 800 and 1200  $\mu\text{m}$  represents the majority of the granules with a percentage of 80%. The second class of about 20% represents granules which size less than 500  $\mu\text{m}$ .

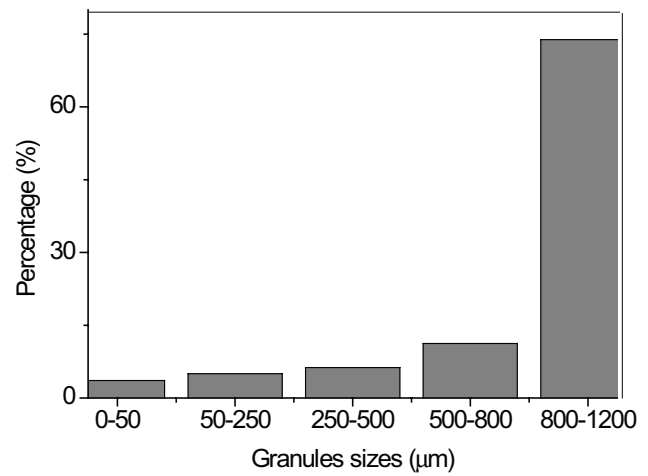


Fig. 2. Granulometric size of Fe-GSMPM sorbents.

Table 2  
Physical properties of the used sorbent

Powder Fe-SMPM	Modal Diameter (mm)	0.13
	Median Diameter $d_{50}$ (mm)	0.047
	Volumetric weight ( $\text{g}/\text{cm}^3$ )	2.11
	Porosity (%)	–
	Potential Zeta (mV)	+22.29
	pH <sub>pzc</sub>	4.42
Granular Fe-GSMPM	Modal Diameter (mm)	1.1
	Median Diameter $d_{50}$ (mm)	0.9
	Volumetric weight ( $\text{g}/\text{cm}^3$ )	1.18
	Porosity (%)	0.56
	Potential Zeta (mV)	+21.53
	pH <sub>pzc</sub>	4.49

In a recent study on the use of silicone as a binder in wet granulation, Cheknane et al. [5] obtained granules with size ranging between 300 and 1200  $\mu\text{m}$  which are close to those obtained in the present study. For various subsequent adsorption tests, we select the following size fraction [800–1200  $\mu\text{m}$ ].

##### 3.1.2. Physical properties

The efficiency of the Fe-GSMPM adsorbent grains depends both on the available specific surface area and on their sizes. Indeed, the adsorption increases as the size decreases. The corresponding physical properties as well as the size distribution of the studied grains are presented in Table 2.

The distribution of the size of the prepared Fe-SMPM grains as well as their densities clearly indicate that the modal diameter values of all the Fe-GSMPM samples studied are close to 1.1 mm.

##### 3.1.3. Friability index and disintegration test

In order to investigate the consistent and the resistant of prepared Fe-GSMPM, friability and disintegration test has

been used to optimize the percentage of necessary amount of gluten in different prepared mixtures.

As shown clearly in Fig. 3 and Table 3, the mechanical resistance and resistant the Fe-GSMPM granules increased with gluten concentration.

The formation and cohesion of these granules takes place only in mixtures containing more than 40 % of gluten, which is also confirmed by their high stability and resistance (see Table 3). These results are in good agreement with some other previously studies [5,25] on the use of silicone in wet granulation. These authors showed that 40% of silicone was required in the formulation of the final granular sorbents.

### 3.1.4. Physico-chemical characterization of the adsorbents

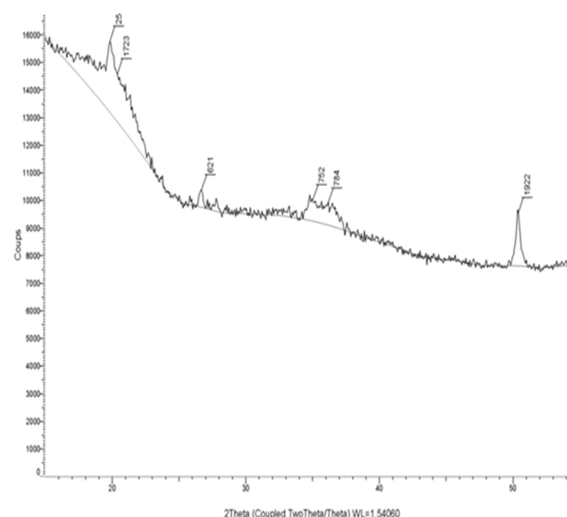
Table 2 presents the zeta potential and the  $pH_{pzc}$  values of all prepared sorbents.

The determination of the surface charge of Fe-GSMPM sorbents allows predicting the different phenomena of sorbate-sorbent interactions. The zeta potential for the granules changed to positive values to reach 22 mV.

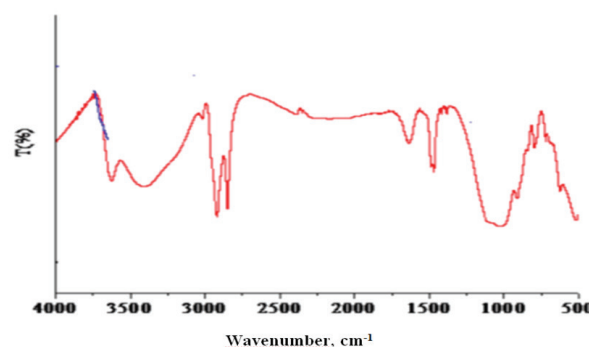
The charge of adsorbent surface is positive at a solution pH lower than that corresponding to the point of zero charge ( $pH_{pzc}$ ) of the surface and is negative at a solution pH

higher than  $pH_{pzc}$ . The value found of  $pH_{pzc}$  was 4.4 for the granules adsorbent.

From XRD patterns (Fig. 4a), interlamellar spacing (d001) increased from 9.6 Å to up to 18 Å after intercalation of the montmorillonite by the pillaring solution and the presence of cetyl trimethyl ammonium and gluten in the pillared clay was confirmed by characteristic bands in the



(a) XRD patterns of the prepared adsorbents



(b) FTIR spectrum of the studied materials.

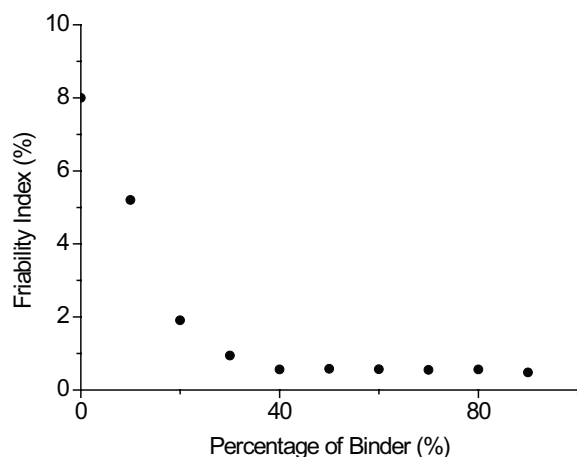
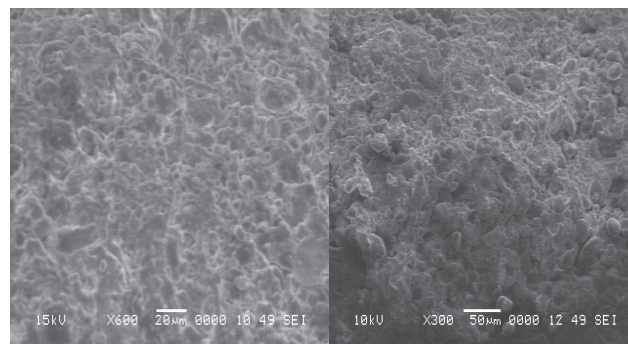


Fig. 3. Friability index of Fe-GSMPM with gluten percentage.

Table 3  
Disintegration test of the prepared Fe-GSMPM

Percentage of gluten (%)	Results of disintegration tests	Cheknane results [5]
10	Disintegration	Disintegration
20	Disintegration	Disintegration
30	Disintegration	Disintegration
40	No Disintegration	No Disintegration
50	No Disintegration	No Disintegration
60	No Disintegration	No Disintegration
70	No Disintegration	No Disintegration
80	No Disintegration	No Disintegration



(c) SEM images.

Fig. 4. Characterization of Fe-GSMPM adsorbent: (a) XRD patterns of the prepared adsorbents, (b) FTIR spectrum of the studied materials, (c) SEM images.

FTIR spectra (Fig. 4b). The cetyl trimethyl ammonium chain seems to be filled completely the micropores, decreased the Specific Surface Area but increased the hydrophobic character (see Table 4). XRD patterns and FTIR spectra showed that the Fe-GSMPM used in this study were well-defined mineral phases.

The morphological characterizations of adsorbents were scanned by SEM and images were presented in (Fig. 4c). The granular surfactant iron pillared montmorillonite were bonded with massive binder fibers in these granular adsorbents which may generate more channels and pores in adsorbents. The result of SEM analysis showed that the gluten was uniformly distributed on the granules adsorbents.

### 3.2. Adsorption studies

#### 3.2.1. Single component systems

##### 3.2.1.1. Kinetic studies

The sorption kinetics of MG and RB at initial concentration of 10 mg/L is shown in Fig. 5. A curves  $q = f(t)$  giving the variation of the adsorption capacity of MG and/or RB vs. time.

According to these curves, adsorption occurs in two distinct phases: an initial rapid phase took about 1 h in which the sorption capacity increases to around (80% for MG and 55% for RB) at equilibrium. This phase is followed by another one in which the solute adsorption rate becomes progressively slower and the pseudo-equilibrium state was reached at about (94% and 64% for MG and RB, respectively).

As shown in comparative study (Fig. 5.), MG molecules were adsorbed faster and well than RB molecules due to differences in molecular structure, solubility and the functional groups.

Indeed, an RB molecule whose molecular weight is higher than that of MG seems to diffuse slowly into the sorbent. This assumption is in perfect agreement with some previously studies [25,41,44].

In order to investigate the mechanism of MG and/or RB adsorption on Fe-GSMPM samples, several kinetic models were applied to the experimental data. The pseudo-first- and pseudo-second-order models were used to specify the adsorption mechanism. The corresponding constant rates  $k_1$

and the correlation coefficients ( $R^2$ ) values are summarized in Table 5. Obtained results showed that the pseudo-first order model ( $R^2 = 0.96$ ) gave the best correlation than the second one ( $R^2 = 0.63$ ).

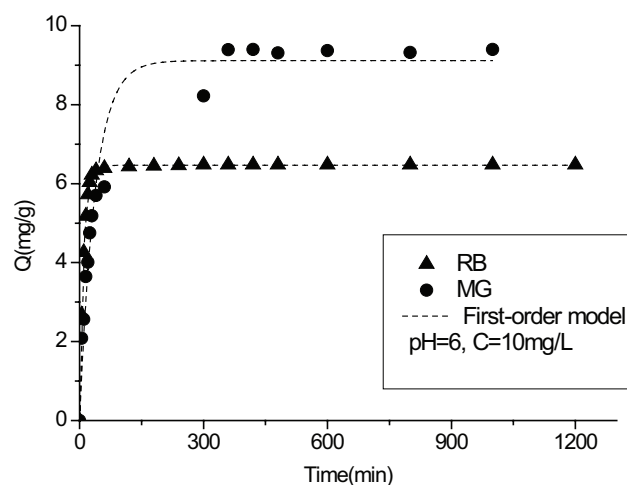


Fig. 5. Pseudo-first-order plot for the adsorption of MG and RB onto Fe-SMPMG.

Table 5  
Pseudo-first-order parameters

		$k_1$ (min <sup>-1</sup> )	$R^2$
MG	alone	$0.097 \pm 0.0055$	0.96
	$r = 9$	$0.069 \pm 0.0050$	0.88
	$r = 3$	$0.206 \pm 0.0392$	0.69
	$r = 1$	$0.092 \pm 0.0130$	0.90
	$r = 1/3$	$0.004 \pm 0.0015$	0.88
	$r = 1/9$	$0.036 \pm 0.0140$	0.40
RB	alone	$0.107 \pm 0.0064$	0.99
	$r = 9$	$0.056 \pm 0.0078$	0.87
	$r = 3$	$0.042 \pm 0.0030$	0.96
	$r = 1$	$0.032 \pm 0.0060$	0.82
	$r = 1/3$	$0.001 \pm 0.0003$	0.96
	$r = 1/9$	$0.004 \pm 0.0004$	0.97

Table 4  
Characterization of the used pillared montmorillonite

Sample	$d_{001}$ (Å) <sup>a</sup>	SSA (m <sup>2</sup> /g)	pHpzc	CEC (meq/100 g)	References
Raw bentonite	14	54		65	Bouras et al. [40]
Na-Mt	15 (9.6 at 200°C)	91	2.60	78	Bouras et al. [40]
Fe-PIM	22	165	4.10	12	Bouras et al. [40]
Fe-SMPM	19.8	14	4.42	7	(This study)
Fe-GSMPM	19.8	14	4.49	7	(This study)
Gluten	17.2	–	6.90	–	(This study)
GIOCs	18.4	–	5.30	–	Cheknane et al. [34]

<sup>a</sup>After thermal treatment; PIM: pillared montmorillonite, Fe-SMPM: iron powder surfactant modified pillared montmorillonite, Fe-GSMPM: iron granular surfactant modified pillared montmorillonite, GIOCs: Granular Pillared Organic Inorganic Clays prepared by Cheknane et al. [34].

### 3.2.1.2. Adsorption isotherms

Adsorption isotherms of MG and RB presented in Fig. 6 were studied in pH 6 with initial concentrations of 10 mg/L and a contact time of 24 h.

In general and according to the adsorption capacities (see Fig. 6) our prepared adsorbent Fe-GSMPM has a high selectivity to MG compared to the RB molecules. Results show clearly that the equilibrium isotherms of the two used dyes onto Fe-GSMPM granules are in close agreement with Freundlich's equation, as the correlation coefficient ( $R^2$ ) values reached 0.9. The isotherm constants were calculated using non-linear regression and their corresponding values are listed in Table 6.

The parameter values of the Freundlich isotherm are greater than unity, indicating that in single-component systems, the MG and RB molecules are preferentially sorbed on the Fe-GSMPM granules through relatively weak bonds between sorbate molecules and surface sites of the sorbent. This indicates that the sorption mechanism appears to be mainly physical [24–25,43].

## 3.2.2. Sorption in binary component systems

### 3.2.2.1. Kinetic studies

Competitive adsorption of MG and RB in binary systems on Fe-GSMPM differed from that in single component systems. Indeed, in simultaneous adsorption, interferences and competition phenomena for sorption sites could occur. The corresponding results presented in Fig. 7 are compared with those obtained in single component systems.

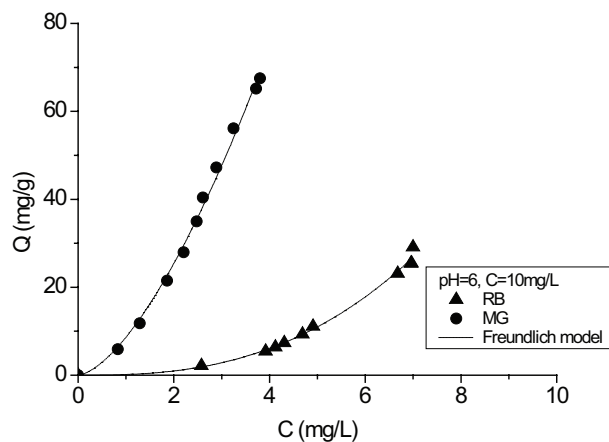


Fig. 6. Sorption isotherms in single component systems fitting with the Freundlich model.

Table 6  
Sorption isotherm constants for dyes sorption on granules

		Freundlich model		
		$K_F$	$N$	$R^2$
MG	pH6	$8.64 \pm 0.57$	$1.55 \pm 0.056$	0.99
RB	pH6	$0.154 \pm 0.038$	$2.65 \pm 0.132$	0.99

Once equilibrium was reached, the adsorption capacity was around 8 mg/g (86%) and 6 mg/g (64%), respectively for MG and RB.

The amount has remained unchanged in comparison with that obtained in single component systems. However, the adsorption capacities of MG were strongly influenced by the presence of RB by reducing their adsorption capacities. Thus, an increase in the concentration of RB in the mixture leads to a decrease of the adsorption of MG.

For all the used weight ratios ( $r = \text{MG}/\text{RB}$ ), obtained values suggest that there is a competition between the MG and RB species towards the same adsorption sites of Fe-GSMPM sorbent. Indeed, the sorption capacities of MG were reduced from 9.4 mg/g (in a single-component system) to 8.6 mg/g (in mixture system). In contrast, the sorption capacities of RB seem to be not influenced by the presence of MG since the value remains constant around 6.4 mg/g both in single and in mixture component systems.

### 3.2.2.2. Isotherms studies

To gain further understanding on the adsorption of MG in the presence of RB, the adsorption experiments were con-

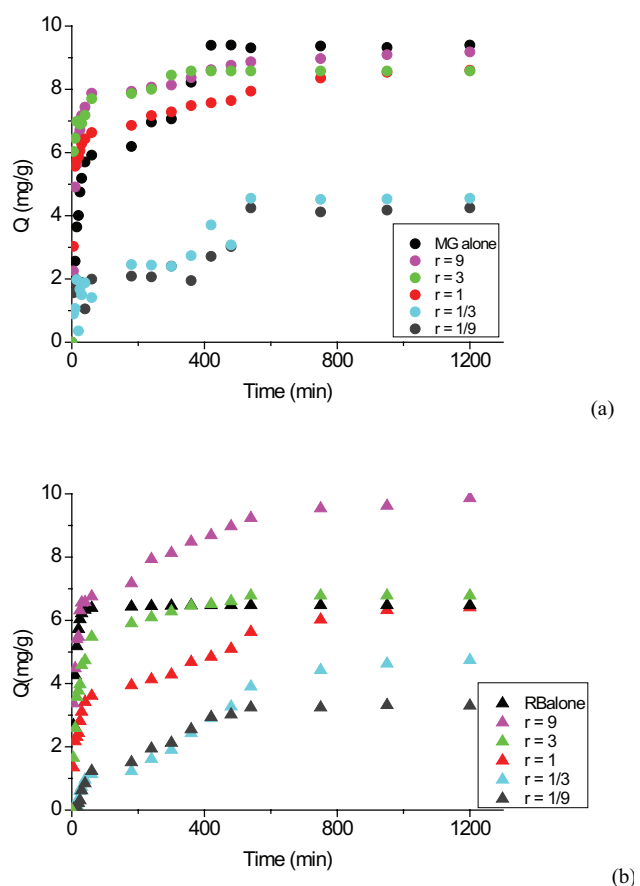


Fig. 7. Kinetic sorption at different weight ratios of MG (a) and RB (b) onto Fe-SMPMG.



ducted at pH 6 and five weight ratios ( $r = \text{MG}/\text{RB}$ : 1/9, 1/3, 1, 3, 9 w/w) and were compared with those obtained in single-component systems.

Based on the curves showed in Fig. 8, the removal efficiency values of MG were around 42%, 45%, 79%, 86%, and 91% while the corresponding values of RB were 33%, 47%, 64%, 68%, and 87% when 1/9, 1/3, 1, 3, and 9, were used as weight ratios, respectively.

The simultaneous adsorption of MG and RB has been fitted by the extended Freundlich model established by Sheindorf et al. [39]. This model, simple and efficient is particularly suitable for binary mixtures that are used in this study.

The competition coefficients  $a_{12}$  and  $a_{21}$  values (see section 2.2.4) at different weight ratios  $r = \text{MG}/\text{RB}$  are listed in Table 7. These coefficients were estimated from the modeling results using the method of non-linear regression.

In the studied range of MG/RB weight ratio  $r$ , an antagonistic effect between MG and RB molecules is clearly appeared since  $a_{12}$  values increased and  $a_{21}$  decreased when  $r$  decreased.

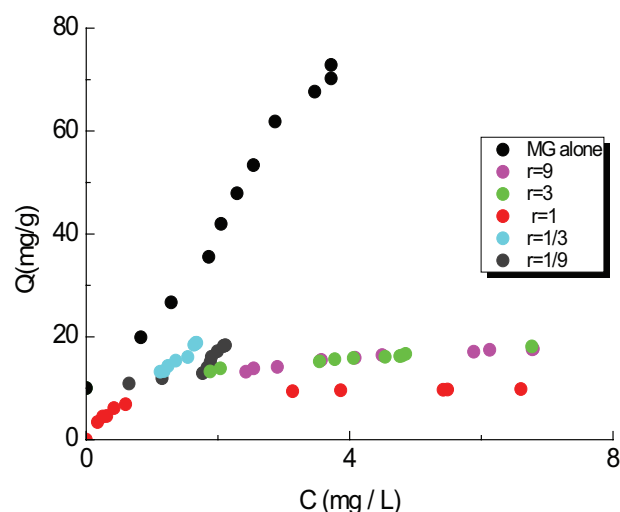


Fig. 8. Adsorption isotherms in mixture systems at pH = 6 and different weight ratios  $r = \text{MG}/\text{RB}$ .

Table 7  
Parameters (SRS) model on the ration weight  $r$  on granules

$r = \text{MG}/\text{RB}$	$a_{12}$	RMSE	$a_{21}$	RMSE
$r = 9$	0.67	40.58	1.49	8.01
$r = 3$	1.24	49.67	0.81	0.99
$r = 1$	1.56	105.33	0.64	23.58
$r = 1/3$	2.44	268.51	0.41	14.01
$r = 1/9$	6.58	651.52	0.15	6.17

The competition coefficients  $a_{12}$  and  $a_{21}$  were determined by running the STATISTICA software with respect the condition  $a_{12} \times a_{21} = 1$

$$\text{RMSE} = \sqrt{\frac{1}{N} \sum_{i=1}^N [Q_{\text{theorique}} - Q_{\text{experimental}}]^2}$$

### 3.3. Sorption mechanism

#### 3.3.1. Effect of granule size

All obtained results both in single component and in binary systems (Fig. 9a) were shown that the sorption capacities strongly depend on the size of the prepared Fe-GSMPM. They show in particular that the granulation process affects both the maximum adsorption capacities and the adsorption rate. Indeed, better sorption capacities (10 mg/g of MG and 8 mg/g of RB) are achieved with the smallest particle sizes (50  $\mu\text{m}$ ) due essentially to their higher contact surfaces.

In single component systems and for all used granular Fe-GSMPM sizes, the sorption capacities of MG (67 mg/g) are slightly greater compared to those obtained with the RB (29 mg/g). In mixture systems and under the used experimental conditions, the uptake of MG on Fe-GSMPM granular is different than that obtained in mono-component single systems.

#### 3.3.2. Effect of pH

As shown in Fig. 9(b) and for all cases, the sorption is favorable at pH above 6 and decreases when pH increases.

At acidic aqueous solution (pH = 3) and when  $\text{pH} < \text{pH}_{\text{pzc}}$  (4.49), the two sorbates exist mainly as cationic forms ( $\text{pH} < \text{pKa}(\text{MG}) = 10$  and  $\text{pKa}(\text{RB}) = 4.42$ ), while the Fe-GSMPM sorbent surfaces are positively charged. This results in electrostatic repulsive interactions, which reduce the adsorption capacity.

The uptake of high quantities of solute depends not only on the adsorbent surface properties but also on the structure of the dye molecules.

Concerning the co-adsorbate RB, the small molecules having sizes of about 0.7 nm also exist as cationic monomer form in acid medium (pH = 3) and thus can easily access the pores of the adsorbent.

At pH = 6 close to neutrality ( $\text{pH} = 6 < \text{pKa}(\text{MG}) = 10$ ,  $\text{pH}_{\text{pzc}}(\text{Fe-GSMPM}) = 4.49$ ), the granules surface is negatively charged ( $\text{pH} > \text{pH}_{\text{pzc}}$ ) and MG cations are adsorbed through strong electrostatic interactions established between the positive cations and the negative charge of adsorbent surface causing an increasing of sorption capacities of about 94 %.

Under the same pH conditions, the RB dye takes the Zwitterionic form with a predominance of the RB cations and the surface sites of the adsorbent become negatively charged ( $\text{pH}_{\text{pzc}} = 4.49$ ). The small adsorbed quantities observed corresponding to an elimination rate of about 64% of RB dye are due to both the repulsive interactions between Zwitterionic form of RB and adsorbent surface of granules as well as to the hydrophobic interactions between the Fe-GSMPM hydrophobic and the cationic species  $\text{RB}^+$  which are themselves hydrophobic.

In mixture systems and at the used conditions (pH = 6 and  $C_0 = 10 \text{ mg/L}$ ), we studied the influence of RB/Mg weight ratio MG/RB in g/g (1/9, 1/3, 1, 3 and 9) on the sorption capacities of Fe-GSMPM in aqueous solution. In such conditions, both MG (pKa = 10) and RB (pKa = 4.42) were almost totally present as cationic species. The simultaneous sorption of these two solutes has been described by

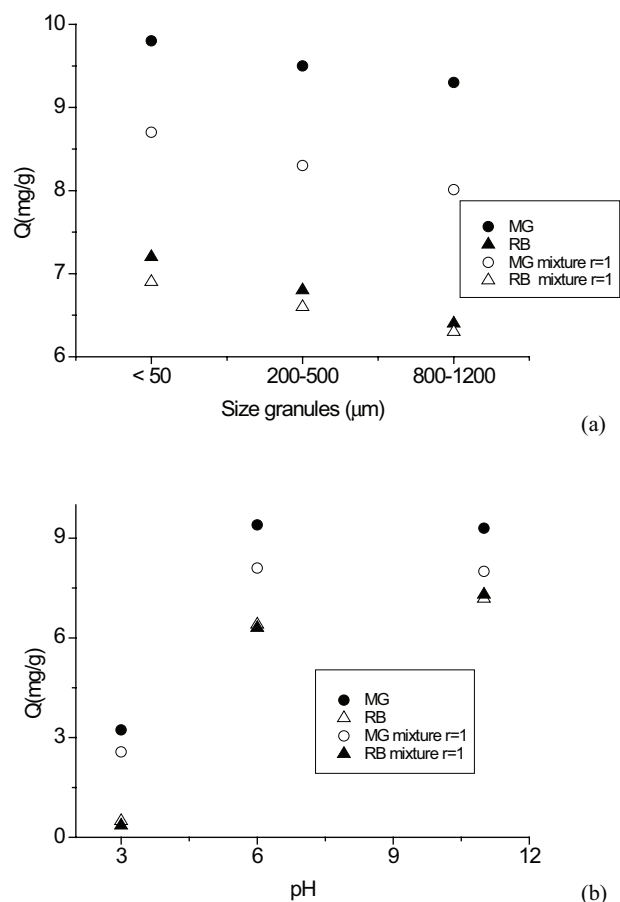


Fig. 9. Effect of granules size (a) and pH (b) on adsorption capacities in single and mixture systems.

the Sheindorf–Rebuhn–Sheintuch (SRS) model (an extended Freundlich model) [39]. The corresponding parameter values  $a_{12}$  and  $a_{21}$  (see section 3.2.2.2) at different weight ratio are shown in Table 7.

Results presented in Fig. 7 were shown that RB defavourably affects the adsorption of MG with a decrease in adsorption from 91% ( $r = 9$ ) to 42% ( $r = 1/9$ ). The sorption efficiency of Fe-GSMPM increases with weight ratio as compared with their properties in a single component system.

This clearly indicates a competition in the adsorption between the two solutes where the cations of the co-adsorbate RB seem to block the adsorption of those of the main MG adsorbate to the same sorbent sites.

In the studied interval of MG/RB ratio competition between MG and RB occurred towards adsorption of Fe-GSMPM. When, the weight ratio  $r$  increases from 1/9 to 9, the competition coefficient values of  $a_{21}$  increases and that of  $a_{12}$  decreases, suggesting that the uptake affinity of MG was lesser than that of RB.

This variation in adsorption can be explained as follows:

An increase in the pH of the medium (from 3 to 6) leads to a decrease in the protonation and to an increase in the adsorption rate suggesting that the sites dedicated to the cationic exchange become more abundant.

So, the protonation of MG molecules occurs in an acidic medium and becomes increasingly deprotonated in basic

medium at high pH values in perfect harmony with suggestions of some previous studies [5,25].

At the studied conditions ( $\text{pH} = 6$ ;  $C_0 = 10 \text{ mg/L}$ ;  $r = \text{MG/RB}: 1/9, 1/3, 1, 3, 9$ ), the MG and RB dyes exist in cationic and Zwitterionic form respectively, while the Fe-GSMPM surfaces is negatively charged. This results in a competition of the cationic species of the two sorbates to the same adsorbent sites through electrostatic forces. For all the selected ratios, the MG adsorption capacities are always greater than the RB.

At this stage of our study, we can therefore conclude note that the adsorption capacities in binary component systems are significantly lower than those obtained when the two solutes are tested separately in single-component systems.

#### 4. Conclusion

In this current work, a laboratory investigation was carried out to prepare coherent and consistent granular sorbents Fe-GSMPM and to evaluate the performance of these granules by the adsorption of two dyes as organic pollutants MG and RB.

The test performed on the sorption of MG and RB in the single and binary component systems showed that Fe-GSMPM is able to effectively retain such compounds.

It was also shown that the pseudo-first-order kinetic fits well with the experimental data. It could be confirmed that MG and RB were mainly retained by physical interactions.

Freundlich isotherm model show best fits with the experimental single component adsorption equilibrium data. A reduce of adsorption capacity of MG in presence of RB was observed. Prediction of the competitive adsorption behavior of the two pollutants indicates that the Sheindorf–Rebuhn–Sheintuch (SRS) model, is able to describe the simultaneous adsorption MG and RB.

The antagonistic effect existing between MG and RB is goodly shown by the interaction coefficients  $a_{12}$ , which decrease with increase of  $r$ .

#### References

- [1] C.O. Plamondon, R.J. Lynch, A. Al-Tabbaa, Comparison between granular pillared organo and inorgano–organo-bentonites for hydrocarbon and metal ion adsorption, *Appl. Clay Sci.*, 67 (2012) 91–98.
- [2] P. Kleinebudde, Roll compaction/dry granulation: pharmaceutical applications, *Euro. J. Pharm. Biopharm.*, 58 (2004) 317–326.
- [3] P. Knight, Challenges in granulation technology, *Powder Tech.*, 140 (2004) 156–162.
- [4] S.M. Iveson, J.D. Litster, K. Hapgood, B.J. Ennis, Nucleation, growth and breakage phenomena in agitated wet granulation processes: a review, *Powder Tech.*, 117 (2001) 3–39.
- [5] B. Cheknane, O. Bouras, M. Baudu, J.P. Basly, A. Cherguielaine, Granular inorgano-organopillared clays (GIOC): Preparation by wet granulation, characterization and application to the removal of a Basic dye (BY28) from aqueous solutions, *Chem. Eng. J.*, 158 (2010) 528–534.
- [6] Z. Belohlav, L. Brenkova, J. Hanika, P. Durdil, P. Rapek, V. Tomasek, Effect of drug active substance particles on wet granulation process, *Chem. Eng. Res. Design.*, 85(A7) (2007) 974–980.
- [7] A. Heim, A. Obraniak, T. Gluba, Changes of feed bulk density during drum granulation of bentonite, *Phys. chem Prob. Mineral Processing*, 39 (2005) 219–228.

- [8] G.I. Kelbaliyev, V.M. Samedli, M.M. Samedov, Modelling of granule formation process of powdered materials by the method of rolling, *Powder Tech.*, 194 (2009) 87–94.
- [9] M.G. Herting, P. Kleinebudde, Studies on the reduction of tensile strength of tablets after roll compaction/dry granulation, *Euro. J. Pharm. Biopharm.*, 70 (2008) 372–379.
- [10] B.X. Thanh, C. Visvanathan, M. Spérandio, R.B. Aim, Fouling characterization in aerobic granulation coupled baffled membrane separation unit, *J. Membr. Sci.*, 318 (2008) 334–339.
- [11] X. He, J. Li, H. Cheng, C. Jiang, C. Wan, Controlled crystallization and granulation of nano-scale B-Ni(OH)<sub>2</sub> cathode materials for high power Ni-MH batteries, *J. Power Sources*, 152 (2005) 285–290.
- [12] Y. Liu, H.L. Xu, S.F. Yang, J.H. Tay, Mechanisms and models for anaerobic granulation in up flow anaerobic sludge blanket reactor, *Water Res.*, 37 (2003) 661–673.
- [13] T. Kapsidou, I. Nikolakakis, S. Malamataris, Agglomeration state and migration of drugs in wet granulations during drying, *Inter. J. Pharm.*, 227 (2001) 97–112.
- [14] V. Landillon, D. Cassan, M.H. Morel, B. Cuq, Flowability, cohesive, and granulation properties of wheat powders, *J. Food Eng.*, 86 (2008) 178–193.
- [15] G. Buelna, Y.S. Lin, Preparation of spherical alumina and copper oxide coated alumina sorbents by improved sol-gel granulation process, *Micropor. Mesopor. Mater.*, 42 (2001) 67–76.
- [16] P. Rajniak, F. Stepanek, K. Dhanasekharan, R. Fan, C. Mancinelli, R.T. Chern, A Combined experimental and computational study of wet granulation in a Wurster fluid bed granulator, *Powder Tech.*, 189 (2009) 190–201.
- [17] S.I. Cantor, S. Kothari, O.M.Y. Koo, Evaluation of the physical and mechanical properties of high drug load formulations: wet granulation vs. novel foam granulation, *Powder Tech.*, 195 (2009) 15–24.
- [18] L.W. H. Pol, S.I.C. Lopes, G. Lettinga, P.N.L. Lens, Anaerobic sludge granulation, *Water Res.*, 38 (2004) 1376–1389.
- [19] A.W.J. Chan, T. Becker, R.J. Neufeld, Subtilisin absorptive encapsulation and granulation, *Proc. Biochem.*, 40 (2005) 1903–1910.
- [20] D. Zhang, J.H. Flory, S. Panmai, U. Batra, M.J. Kaufman, Wettability of pharmaceutical solids: its measurement and influence on wet granulation, *Col. Surf A: Phys. Chem. Eng. aspects.*, 206 (2002) 547–554.
- [21] F. Medici, L. Piga, G. Rinaldi, Behaviour of polyalinophenolic additives in the granulation of lime and fly-ash, *Waste Manage.*, 20 (2000) 491–498.
- [22] M. Bardin, P.C. Knight, J.P.K. Seville, On control of particle size distribution in granulation using high-shear mixers, *Powder Tech.*, 140 (2004) 169–175.
- [23] N. Passerini, B. Albertini, M.L. Gonzalez-Rodriguez, C. Cavallari, L. Rodriguez, Preparation and characterization of ibuprofen-poloxamer 188 granules obtained by melt granulation, *Euro. J. Pharm. Sci.*, 15 (2002) 71–78.
- [24] M. Lezehari, M. Baudu, O. Bouras, J.P. Basly, Fixed-bed column studies of pentachlorophenol removal by use of alginate-encapsulated pillared clay micro beads, *J. Colloid Interface Sci.*, 379 (2012) 101–106.
- [25] B. Cheknane, M. Baudu, J.P. Basly, O. Bouras, F. Zermane, Modelling of basic green 4 dynamic sorption onto granular organo-inorgano pillared clays (GOICs) in column reactor, *Chem. Eng. J.*, 209 (2012) 7–12.
- [26] E.M. Holt, The properties and forming of catalysts and absorbents by granulation, *Powder Tech.*, 140 (2004) 194–202.
- [27] M.K. Tiwari, S. Guha, C.S. Harendranath, S. Tripathi, Enhanced granulation by natural ionic polymer additives in UASB reactor treating low-strength wastewater, *Water Res.*, 39 (2005) 3801–3810.
- [28] H.S. Tan, A.D. Salman, M.J. Hounslow, Kinetics of fluidized bed melt granulation I: The effect of process variables, *Chem. Eng. Sci.*, 61(2006) 1585–1601.
- [29] K.P. Hapgood, B.K. Mohammadi, Granulation of hydrophobic powders, *Powder Tech.*, 189 (2009) 253–262.
- [30] O. Planinsek, R. Pisek, A. Trojak, S. Srcic, The utilization of surface free-energy parameters for the selection of a suitable binder in fluidized bed granulation, *Inter. J. Pharm.*, 207 (2000) 77–88.
- [31] M. Hemati, R. Cherif, K. Saleh, V. Pont, Fluidized bed coating and granulation: influence of process-related variables and physicochemical properties on the growth kinetics, *Powder Tech.*, 130 (2003) 18–34.
- [32] C. Pagnoux, N. Tessier-Doyen, A. Pringuet, M. Cerbelaud, P. Garcia-Perez, Influence of the suspension flocculated state on the microstructure of alumina spheres elaborated by colloidal granulation, *J. Eur. Ceramics Soc.*, 29 (2009) 1379–1385.
- [33] L. Chen, H.X. Wu, T.J. Wang, Y. Jin, Y. Zhang, X.M. Dou, Granulation of Fe-Al-Cenano-adsorbent for fluoride removal from drinking water by spray coating on sand in a fluidized bed, *Powder Tech.*, 193 (2009) 59–64.
- [34] B. Cheknane, F. Zermane, M. Baudu, O. Bouras, J.P. Basly, Sorption of basic dyes onto granulated pillared clays: Thermodynamic and kinetic studies, *J. Colloid Interface Sci.*, 381 (2012) 158–163.
- [35] J.B. Wade, G.P. Martin, D.F. Long, Controlling granule size through breakage in a novel reverse-phase wet granulation process: the effect of impeller speed and binder liquid viscosity, *Inter. J. Pharm.*, 478 (2015) 439–446.
- [36] S. Oka, O. Kašpar, V. Tokárová, K. Sowrirajan, H. Wu, M. Khan, F. Muzzio, F. Štěpánek, R. Ramachandran, A quantitative study of the effect of process parameters on key granule characteristics in a high shear wet granulation process involving a two component pharmaceutical blend, *Adv. Powder Tech.*, 26 (2015) 315–322.
- [37] B.C. Xue, T. Liu, H. Huang, E.B. Liu, The effect of the intimate structure of the solid binder on material viscosity during drum granulation, *Powder Tech.*, 253 (2014) 584–589.
- [38] R. Jing, L. Nan, L. Lei, A.J. Kun, Z. Lin, R. Nan-Qi, Granulation and ferric oxides loading enable biochar derived from cotton stalk to remove phosphate from water, *Biores. Tech.*, 178 (2015) 119–125.
- [39] C. Sheindorf, M. Rebhun, M. Sheintuch, A Freundlich-type multicomponent isotherm, *J. Colloid Interface Sci.*, 79 (1981) 136–142.
- [40] O. Bouras, J.C. Bollinger, M. Baudu, Effect of humic acids on pentachlorophenol sorption to cetyl-trimethyl-ammonium-modified, Fe- and Al-pillared montmorillonites, *Appl. Clay Sci.*, 50 (2010) 58–63.
- [41] V. Lenoble, O. Bouras, V. Deluchat, B. Serpaud, J.C. Bollinger, Arsenic adsorption onto pillared clays and iron oxides, *J. Colloid Interface Sci.*, 255 (2002) 52–58.
- [42] F. Zermane, O. Bouras, M. Baudu, J.P. Basly, Cooperative coadsorption of 4-nitrophenol and basic yellow 28 dye onto an iron organo-inorgano pillared montmorillonite clay, *J. Colloid Interface Sci.*, 350 (2010) 315–319.
- [43] F. Zermane, B. Cheknane, J.P. Basly, O. Bouras, M. Baudu, Influence of humic acids on the adsorption of Basic Yellow 28 dye onto an iron organo-inorgano pillared clay and two hydrous ferric oxides, *J. Colloid Interface Sci.*, 395 (2013) 212–216.
- [44] S. Hamidouche, O. Bouras, F. Zermane, B. Cheknane, M. Houari, J. Debord, M. Harel, J.C. Bollinger, M. Baudu, Simultaneous sorption of 4-nitrophenol and 2-nitrophenol on a hybrid geocomposite based on surfactant-modified pillared-clay and activated carbon, *Chem. Eng. J.*, 279 (2015) 964–972.